Environ Monit Assess (2022) 194: 302
https://doi.org/10.1007/s10661-022-09964-z

Comparison of reactive azo dye removal with UV/H_2O_2, UV/$S_2O_8^{2-}$ and UV/HSO_5^- processes in aqueous solutions

Kübra Çobanoğlu · Nejdet Değermenci

Received: 18 November 2021 / Accepted: 19 March 2022 / Published online: 28 March 2022

Abstract Advanced oxidation processes (AOPs) are an effective choice for removal of reactive azo dyes used in the textile industry due to high solubility and low degradability. Within the scope of this study, reactive orange 122 (RO122) azo dye was removed using the UV-based AOPs of ultraviolet (UV) radiation, UV/hydrogen peroxide (UV/H_2O_2), UV/persulfate (UV/$S_2O_8^{2-}$), and UV/peroxymonosulfate (UV/HSO_5^-). Oxidant concentration, initial solution pH, initial RO122 concentration, different anions (Cl^-, NO_3^- and SO_4^{2-}), and solution temperature effects were compared. With only UV radiation (254 nm), 19.5% RO122 removal occurred at the end of 120 min. The RO122 removal reduced with the UV/oxidant processes at pH 9. Experimental results revealed RO122 removal followed pseudo-first-order (PFO) kinetics. There was a linear correlation identified between initial oxidant concentration and the PFO kinetic rate constant (k_1). Among the three UV-based processes, with oxidant concentration 50 mg/L, temperature 20 °C, and pH 5, RO122 removal efficiency was in the order UV/H_2O_2 > UV/HSO_5^- > UV/$S_2O_8^{2-}$. RO122 removal rate increased as initial oxidant concentration and temperature increased and reduced as initial RO122 concentration increased. Energy requirements and oxidant costs were assessed. The UV/H_2O_2 process was concluded to be the most efficient and economic process for RO122 removal.

Keywords Decolorization · Reactive orange 122 · Azo dye · Advanced oxidation processes · Kinetics · Cost analysis

K. Çobanoğlu · N. Değermenci (✉)
Kastamonu University, Kastamonu, Turkey
e-mail: ndegermenci@gmail.com

Introduction

A global increase in population and the continuous and rapid development of industrial practices have resulted in increased health risks due to environmental pollution. Wastewater from the activities of various industries such as textiles, paper, food, pharmaceuticals, plastic, cosmetics, and tanning contain synthetic dyes that negatively affect the environment; this situation continues to be a significant global problem in the present day (De Gisi & Notarnicola, 2017; Mahmoud et al., 2021). The textile industry uses more than 50% of these synthetic dyes; wastewater from industrial activities associated with textiles contains refractory dyes that have varying degrees of toxicity which can potentially remain in the environment for long periods (Kishor et al., 2021; Peng et al., 2008; Yang et al., 2011). These synthetic dyes can be classified based on the chemical structure of their chromophore groups (Rodrigues de Almeida et al., 2019). Azo dyes represent more than half of the synthetic dyes used in the paint industry due to their lower cost, higher stability, anLE: Keywords are required. Please provide.d diverse range of colors, making them

the most commonly used class of dye across the world (Cui et al., 2016; Ravadelli et al., 2021). However, large amounts of azo dyes are present in wastewater due to the inefficiency of the dyeing processes (Azam & Hamid, 2006). About 10–50% of these refractory dyes are discharged into wastewater as a result of the dyeing process (Blackburn, 2004). These wastewaters are discharged pre-existing water masses and represent a threat to the ecosystems within these environments. They can cause anoxic conditions which negatively affect both fauna and flora, reduce the penetration depth of sunlight, negatively affect photosynthetic activity, and reduce the concentration of dissolved oxygen (Adar, 2021; Cao et al., 2019; Zhan et al., 2020). Thus, the use of effective treatment methods to degrade any dyes contained within the wastewaters produced by the dyeing process is of great importance.

Azo dyes are known to be problematic chemicals in textile industry wastewaters due to their high solubility and low degradability (Malakootian et al., 2015; Pérez-Calderón et al., 2020). Many synthetic azo dyes and metabolites are toxic, carcinogenic, and mutagenic and thus pose significant health risks for humans (Balapure et al., 2015; Saratale et al., 2009). Hence, industrial wastewaters containing azo dyes and their metabolites must be treated before they are discharged into the environment. There are many methods of removing dyestuffs from textile wastewaters, such as active carbon adsorption, chemical coagulation/precipitation, electrochemical oxidation, membrane filtration, chemical oxidation, biological degradation, and advanced oxidation processes (AOPs) (Değermenci, 2021; Meerbergen et al., 2017; Santos & Boaventura, 2016; Sirajudheen et al., 2020). Although biological treatment is the most common treatment method owing to the minimal effect it has on the environment as well as its cost-efficiency, traditional wastewater treatment processes involving active sludge cannot fully degrade due to the stability and xenobiotic structure of reactive azo dyes (Ganesh et al., 1994; Pearce et al., 2003; Ravadelli et al., 2021). Despite being easily reduced under anaerobic conditions, azo dyes create potentially hazardous aromatic amines during anaerobic degradation (Franca et al., 2020; Peng et al., 2008). Chemical coagulation/precipitation treatments generally have high operational costs and generate chemical sludge (Kausar et al., 2021). Active carbon adsorption is expensive and not commercially attractive and merely converts pollutants from one phase to another (Alaton et al., 2002; Guo et al., 2012). Thus, there is a need for new and more efficient technologies for the treatment of reactive azo dyes in wastewater. Due to the limitations of traditional processes, AOPs based on very reactive species like hydroxyl and/or sulfate radicals are new and potentially suitable methods of removing dyeing agents from wastewater (Kermani et al., 2020). In addition, the increasing water quality requirements for the reuse of wastewater, as well as the intensification of discharge regulations, have resulted in the increased application of AOPs for wastewater treatment on an industrial scale (Bakht Shokouhi et al., 2020; Zhang et al., 2016).

Ultraviolet (UV)-based AOPs have been accepted as an alternative to traditional water/wastewater treatment processes due to their ability to create highly reactive free radicals, such as hydroxyl and/or sulfate radicals (Khan et al., 2014; Klavarioti et al., 2009; Zhang et al., 2016). UV-based technologies are simple, clean, relatively cheap, and are generally more efficient than chemical AOPs. In addition, these methods may disinfect water and can be used for the removal of pollutants (Oturan & Aaron, 2014). Hydrogen peroxide (H_2O_2), persulfate ($S_2O_8^{2-}$), and peroxymonosulfate (HSO_5^-) are the oxidizing agents used in the removal of organic pollutants (Dhaka et al., 2018; Liu et al., 2016; Qi et al., 2016). These compounds have a similar structure, and they all contain O–O bonds. H_2O_2 has the highest bond energy at 213.3 kJ/mol, while $S_2O_8^{2-}$ has a predicted bond energy of 140 kJ/mol. No value for the bond energy of HSO_5^- could be found in the literature; however, it is stated that the bond energy of HSO_5^- may be between $S_2O_8^{2-}$ and H_2O_2 (Kolthoff & Miller, 1951; Yang et al., 2011). Each of these compounds is limited in its ability to independently oxidize organic matter. However, they can create hydroxyl and/or sulfate radicals in the presence of UV. Under appropriate conditions, H_2O_2 is considered to be an environmentally friendly oxidizing agent as its final transformation products, such as water or hydroxyl ions, are environmentally safe. As a result, H_2O_2 has drawn a significant amount of attention in "green" chemistry and "green" engineering applications (Dionysiou et al., 2004). The combination of UV with H_2O_2 was successfully applied to the removal of different pollutants in water (Azam & Hamid, 2006; Zhang et al., 2016). In addition, H_2O_2 is the most common oxidant used to create reactive hydroxyl radicals ($E^0 = 1.9–2.7$ V) (Li et al., 2017). Similarly, the

sulfate radical is highly efficient at removing organic pollutants. Both $S_2O_8^{2-}$ and HSO_5^- can be activated by UV and are used to create sulfate radicals (Siegrist et al., 2011). The sulfate radical ($E^0 = 2.5–3.1$ V) is very reactive and can easily degrade organic compounds; hence, it is commonly used in the removal of many different organic pollutants (Cai et al., 2021; Lee et al., 2021; Liu et al., 2020; Zhang et al., 2014).

Within the scope of this study, the removal efficiency for reactive orange 122 (RO122) was assessed and compared using direct UV radiation, UV/H_2O_2, UV/$S_2O_8^{2-}$, and UV/HSO_5^- processes in a batch reactor. The effects of oxidant concentration, initial solution pH, initial pollutant concentration, different anions (Cl^-, NO_3^-, and SO_4^{2-}), and temperature were systematically researched. Finally, the total treatment cost per order was analyzed with the aim of showing the cost-efficiency of the three treatment processes. The results of this study contain significant practical suggestions for the application of UV-based AOPs in control of the discharge of RO112 into the receiving water environment.

Materials and methods

Chemicals and analysis

Hydrogen peroxide (H_2O_2, 30%) was purchased from J.T.Baker. Potassium persulfate ($K_2S_2O_8$, > 99%) and potassium peroxymonosulfate ($2KHSO_5.KHSO_4.K_2SO_4$, ≥ 4.5% (active oxygen)) were purchased from Acros Organics. Sodium nitrate ($NaNO_3$, ≥ 99%), sodium sulfate (Na_2SO_4, ≥ 99%), sodium chloride (NaCl, ≥ 99%), sodium hydroxide (NaOH, > 99%) and sulfuric acid (H_2SO_4, ≥ 95%) were obtained from Sigma-Aldrich. Potassium iodide (KI, > 99%) and potassium iodate (KIO_3, > 99%) were purchased from Tekkim (Turkey). All of the chemicals were used without additional purification.

RO122 had commercial purity and the chemical structure is given in Fig. 1 (Ferreira et al., 2019). RO122 concentrations were determined using a calibration curve prepared for the maximum wavelength (484 nm) using a spectrophotometer (HachLange, DR6000). Solution pH was measured with a WTW brand (Multi 3620 IDS) mobile digital pH meter. Analysis of samples taken during the reaction duration (RO122 concentration) was completed immediately. RO122 removal efficiency was calculated with the following equation (Eq. (1)).

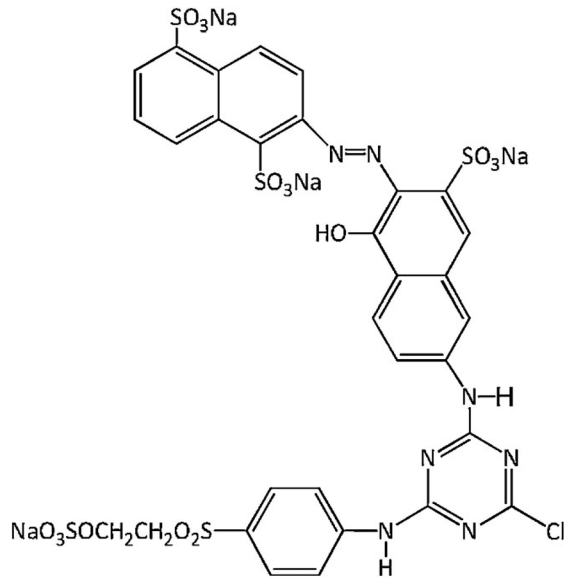

Fig. 1 Chemical structure of RO122

$$\text{Removal}\,(\%) = \left(1 - C_t/C_0\right) \times 100 \quad (1)$$

Here, C_0 (mg/L) is the initial RO122 concentration while C_t (mg/L) represents the RO122 concentration at time t.

Experimental setup and procedures

Experiments used a cylindrical jacketed reactor with internal diameter 6 cm and height 32 cm. A low-pressure mercury-steam lamp (LightTech, GPH 212T5/L4 10 W, 254 nm) was placed in a quartz sleeve aligned on the same axis as the reactor (Fig. 2). The volume of solutions used in the experiments was 600 mL. Temperature was controlled by a heating–cooling circulator (Labo, C200-H13). A magnetic stirrer (JeioTech, TS-14S) was used at 600 rpm mixing rate to ensure homogeneity of solutions. The pH values were measured using a pH meter (WTW, Multi 3620 IDS). Before the lamp was placed in the quartz bulb, it was allowed to stand for 15 min to reach a constant light intensity. In addition, all outsides of the reactor were covered with aluminum foil so that there will be no loss from the light source. The photon flux entering the solution was measured by the KI/KIO_3 actinometer method (Bolton et al., 2011) as 1.9912 μ Einstein/s.

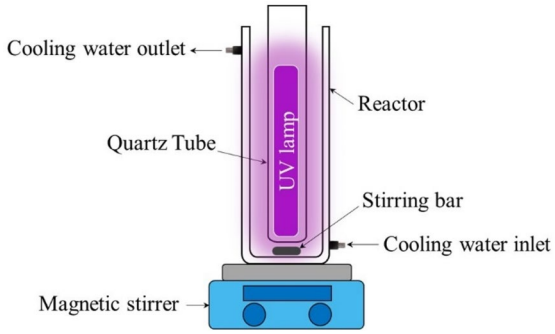

Fig. 2 Experimental setup

Before starting the experiments, the reactor was filled with 600 mL of RO122 aqueous solution at the desired concentration. The pH values of the solutions were adjusted with 0.1 M NaOH or H_2SO_4 solutions. No buffer solution was used in all the experiment to keep the pH constant. After the pH adjustment, the desired amounts of oxidant (H_2O_2, $S_2O_8^{2-}$ or HSO_5^-) were added to the reactor. Samples were removed at previously determined time intervals (i.e., 0, 5, 10, 15, 20, 30, 45, 60, 75, 90, 105, 120 min) and immediately analyzed. Sample solutions were prepared using deionized water. All the experiments were performed in duplicate, and arithmetic average was taken. The effects of different operating parameters such as oxidant concentration ($[H_2O_2]=[S_2O_8^{2-}]=[HSO_5^-]=$50–200 mg/L), RO122 concentration (50–200 mg/L), solution pH (3.0–9.0), and solution temperature (10–40 °C) were elucidated in later sections.

Kinetic analysis

Removal of organic compounds by AOPs generally follows PFO kinetics (Chen et al., 2018; He et al., 2014). The derived visible rate constant (k_1) shows the rate for the whole reaction to a degree. For this reason, the PFO kinetic model (Eq. (2)) was adopted in this study to mimic the RO122 removal kinetics under a variety of reaction conditions.

$$dC/dt = -k_1 C \tag{2}$$

Here, k_1 (min^{-1}) is the rate constant for the PFO kinetic model; t is the reaction duration; and C (mg/L) is the RO122 concentrations at time t. The Microsoft Excel solver plugin tool was used to estimate the kinetic model parameters with non-linear regression.

Economic comparison

The efficiency of AOPs using UV radiation for pollutant removal may be measured with the electrical energy per order (EE/O) proposed by the Photochemistry Commission of the International Union of Pure and Applied Chemistry (IUPAC). This is defined as "the electrical energy in kilowatts per hour (kWh) required to degrade the contaminant by one order of magnitude in 1 m^3 of contaminated water or air" (Bolton et al., 2001). The total for electrical energy and oxidant costs was taken as the basis for economic comparison of the UV/H_2O_2, UV/$S_2O_8^{2-}$, and UV/HSO_5 processes for RO122 removal. Electrical energy costs may be calculated according to Eq. (3), and here, electricity cost used 0.08 $/kWh. For UV-based AOPs, the electrical energy of the UV lamp (EE/O_{UV}) for the batch reactor may be expressed as in Eq. (4). The oxidant costs affecting total cost were 0.051 $/mol for H_2O_2, 0.176 $/mol for persulfate and 0.6762 $/mol for peroxymonosulfate (Zhang et al., 2014). The total cost may be calculated with Eq. (5) with the total for electrical energy costs and oxidant costs:

$$\begin{aligned} \textit{Electrical energy cost} = {} & EE/O_{UV}\ (kWh/m^3/order) \\ & \times \textit{electricity cost}\ (\$/kWh) \end{aligned} \tag{3}$$

$$EE/O_{UV} = \frac{P \times t \times 1000}{V \times \log \times (C_0/C_t)} = \frac{38.4 \times P}{V \times k_1} \tag{4}$$

$$Cost\ /O_{\text{total}}\left(\$\ /m^3/\text{order}\right) = \text{electrical energy cost} + \text{oxidant cost} \tag{5}$$

where P is the UV lamp power (kW); t is the irradiation time (h); V is the reactor volume (L); k_1 is the PFO kinetic rate constant (min^{-1}); C_0 is the initial concentration of RO122 (mg/L); and C_t is concentration at time t (mg/L).

Results and discussion

Removal of RO122 by UV, UV/H_2O_2, UV/$S_2O_8^{2-}$, and UV/HSO_5^- processes

The comparative removal of RO122 with UV/H_2O_2, UV/$S_2O_8^{2-}$, and UV/HSO_5^- processes was investigated, and the results are given in Fig. 3. Control experiments

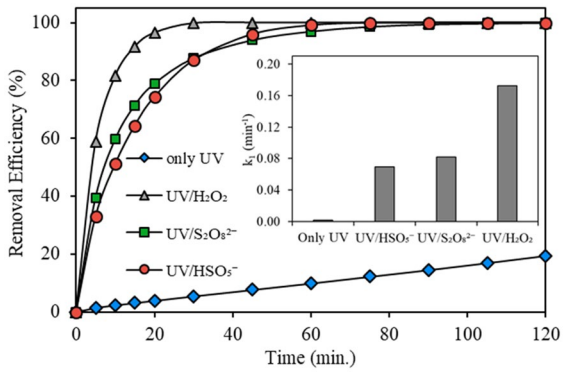

Fig. 3 RO122 removal with UV/H_2O_2, $UV/S_2O_8^{2-}$, and UV/HSO_5^- processes. Experimental conditions: RO122 = 50 mg/L, oxidant = 50 mg/L, pH = 7, T = 20 °C

were performed with the use of H_2O_2, $S_2O_8^{2-}$, and HSO_5^- alone for RO122 removal (in a dark environment) and during 120 min, RO122 removal was not observed with 50 mg/L concentration of these oxidants and pH 7. Due to the presence of π-bonds in the dye molecules, removal may be expected with UV radiation (Rehman et al., 2018). For this reason, RO122 removal was researched using only UV in order to accurately assess the role of oxidants. With only UV radiation, at the end of 120 min, 19.5% RO122 removal occurred. This removal is attributed to direct UV radiation of organic compounds (Beltrán et al., 1997). Similar results were reported for the removal of brilliant green, thiamphenicol, and sulfamethoxazole (Ao & Liu, 2017; Rehman et al., 2018; Wang et al., 2017). As a result of the combination (activation) of H_2O_2, $S_2O_8^{2-}$, and HSO_5^- with UV, reactive species formation occurs linked to the reactions given in Eqs. (6–8), and these reactive species significantly increase RO122 removal. At the end of 30 min using UV/H_2O_2, $UV/S_2O_8^{2-}$, and UV/HSO_5^- processes, 99.8%, 87.7%, and 87.0% RO122 removal was observed, respectively. At the end of 120 min, RO122 was completely removed with all three processes. As a result, the synergistic effect of UV radiation and chemical oxidants affected removal performance by a notable degree. When the UV/H_2O_2 process is compared with the $UV/S_2O_8^{2-}$ and UV/HSO_5^- processes, the reaction duration for full degradation was clearly shorter and this proves that the UV/H_2O_2 process displayed better performance than the $UV/S_2O_8^{2-}$ and UV/HSO_5^- processes. The PFO kinetic rate constants for the three processes were ranked $UV/H_2O_2 > UV/S_2O_8^{2-} > UV/HSO_5^-$ and the equivalent values were 0.1721, 0.0819, and 0.0695 min^{-1}.

$$H_2O_2 + h\nu \rightarrow 2HO^{\bullet} \quad (6)$$

$$S_2O_8^{2-} + h\nu \rightarrow 2SO_4^{\bullet -} \quad (7)$$

$$HSO_5^- + h\nu \rightarrow HO^{\bullet} + SO_4^{\bullet -} \quad (8)$$

Effect of initial solution pH

Solution pH has two important roles for removal efficiency. Firstly, the active oxidation species in solution are largely affected by the solution pH value (Ding et al., 2017; Liang et al., 2007). Secondly, organic compounds convert to different forms according to the specific pKa values for different solution pH values, and this causes different reactivity against radical species (Zhao et al., 2013). For these reasons, the solution pH value is an important parameter for the UV radiation process. Results for RO122 removal linked to reaction duration for experiments performed with different initial pH values are shown in Fig. 4. The removal of RO122 with UV/H_2O_2 and $UV/S_2O_8^{2-}$ processes can be said to be linked to the initial pH value. For all three processes at the end of 120 min, RO122 was fully removed at all initial pH values. The reaction kinetic models were calculated using non-linear methods for the PFO and pseudo-second-order (PSO) kinetic models. All three processes followed the PFO kinetic model at all pH values. The removal of RO122 was inhibited at initial pH 9 for the UV/H_2O_2 process. This was probably due to the reduction of oxidation power of hydroxyl radical (Zhang et al., 2016). In addition, alkaline condition would enhance the reaction of hydroxyl ion and hydroxyl radical (Eq. 9). In the $UV/S_2O_8^{2-}$ process, in acidic and neutral solutions, RO122 removal rate remains approximately constant but then, in basic solutions it significantly decreases. As seen in Fig. 4c, it is seen that the initial pH value and RO122 removal nearly did not change in the UV/HSO_5^- process. Related to the increasing pH value, the kinetic rate constants of PFO are 0.0648, 0.0724, 0.0695, and 0.0692 min^{-1}, respectively (Fig. 4d). However, when the PFO kinetic rate constant values were calculated using the non-linear method, the initial pH

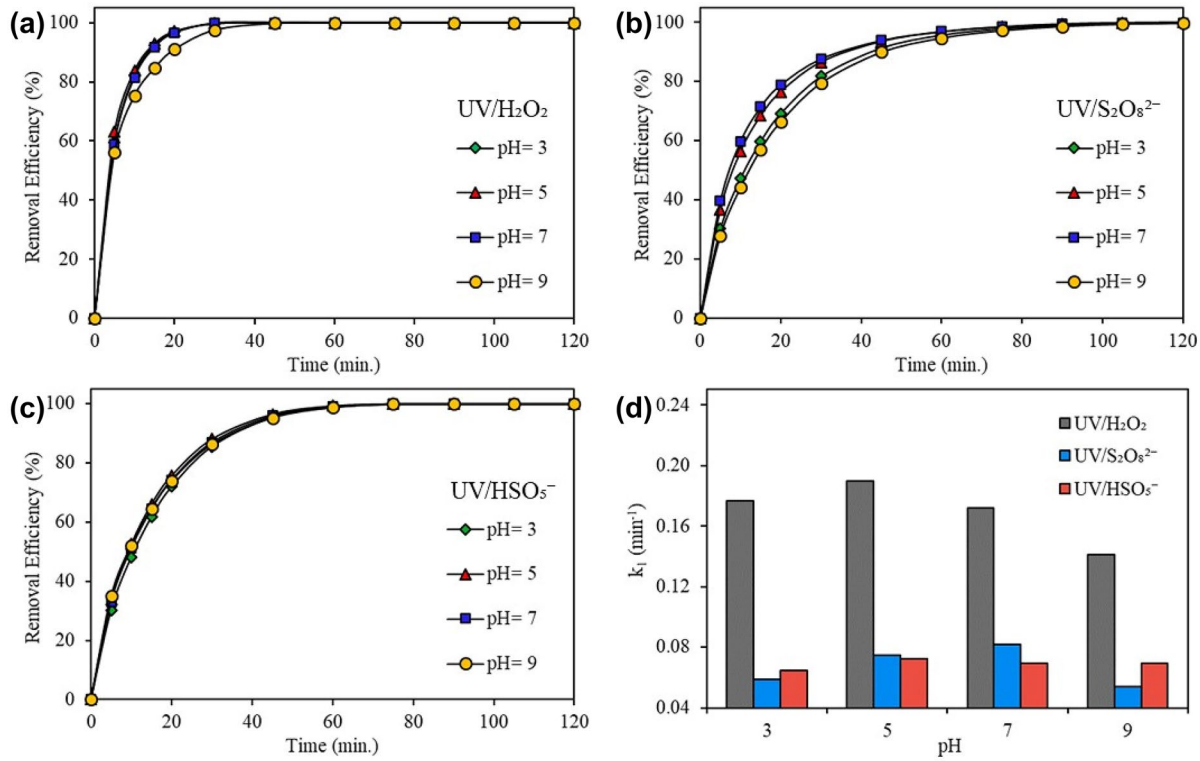

Fig. 4 Effect of pH on RO122 removal. **a** UV/H_2O_2, **b** $UV/S_2O_8^{2-}$, **c** UV/HSO_5^-, and **d** the comparison of PFO kinetic rate constant. Experimental conditions: RO122 = 50 mg/L, oxidant = 50 mg/L, T = 20 °C

value was found to be 5 for the highest kinetic constant obtained. In the UV/HSO_5^- process, the removal rate of RO122 remains approximately constant in acidic and basic solutions. The highest PFO kinetic rate constant value for the UV/H_2O_2 process was at pH 5 (0.1897 min^{-1}) and for the $UV/S_2O_8^{2-}$ process at pH 7 (0.0819 min^{-1}). Generally, pH values of 5 and 7 were more productive for all three processes. With the aim of comparison, the optimum pH value of 5 was chosen for all later experiments.

$$HO^{\bullet} + OH^- \rightarrow H_2O + O^{\bullet -} \quad (9)$$

Effect of initial dye concentration

The effects of initial RO122 concentration on UV/H_2O_2, $UV/S_2O_8^{2-}$, and UV/HSO_5^- processes were investigated linked to time and the results are given in Fig. 5. Experiments had temperature 20 °C, initial pH value 5, and initial oxidant concentration of 50 mg/L. For each of the three processes with initial RO122 concentration of 50 mg/L, full removal occurred at the end of 120 min. With the increase of RO122 concentration to 200 mg/L, removal efficiency reduced and was determined as 68.2%, 31.2%, and 58.0% for UV/H_2O_2, $UV/S_2O_8^{2-}$, and UV/HSO_5^- processes. When removal efficiencies were ranked for initial RO122 concentration of 50 mg/L, the order was $UV/H_2O_2 > UV/S_2O_8^{2-} > UV/HSO_5^-$. For values with initial RO122 concentration above 50 mg/L, the order was $UV/H_2O_2 > UV/HSO_5^- > UV/S_2O_8^{2-}$. Similarly, the reaction rate constant values reduced with the increase in initial RO122 concentration, and the highest reaction rate constant value (0.1897 min^{-1}) was obtained for the UV/H_2O_2 process. The lowest reaction rate constant value (0.0031 min^{-1}) was obtained for the $UV/S_2O_8^{2-}$ process. The reaction rate constants in the three AOPs were correlated exponentially with decreasing initial RO122 concentration. This situation could be attributed to two possible reasons. Firstly, as

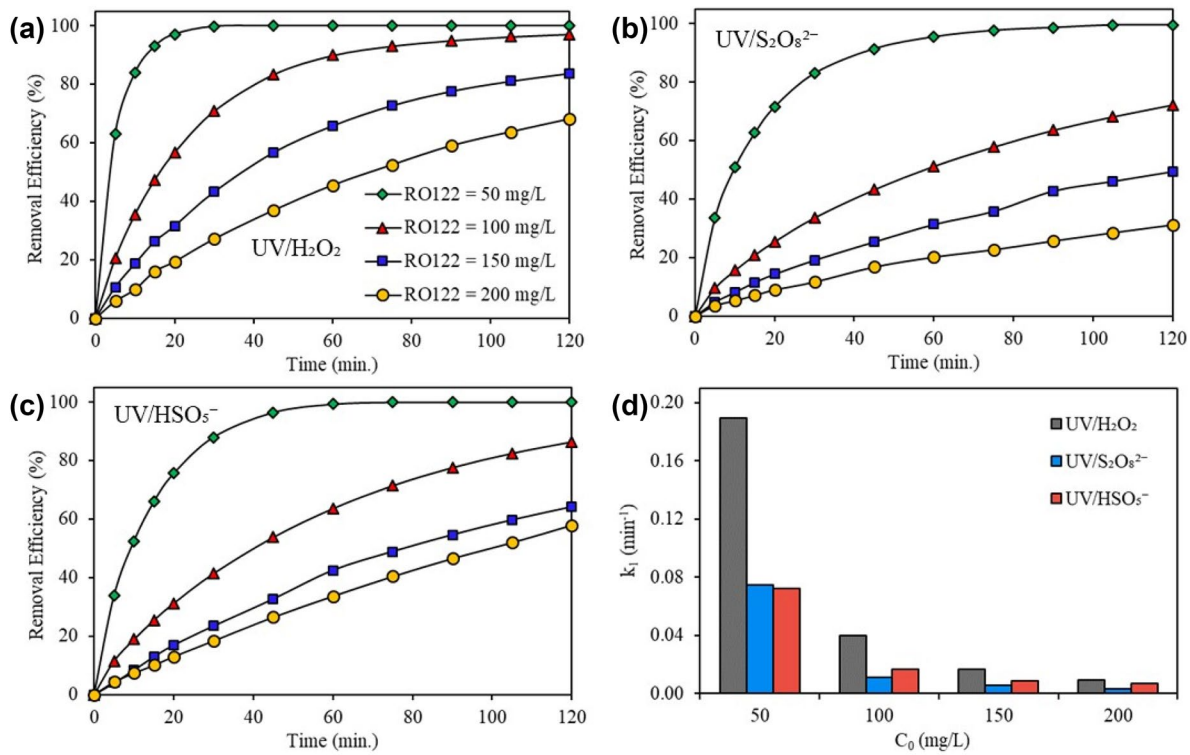

Fig. 5 Effect of initial RO122 concentration on RO122 removal. **a** UV/H_2O_2, **b** $UV/S_2O_8^{2-}$, **c** UV/HSO_5^-, and **d** the comparison of PFO kinetic rate constant. Experimental conditions: pH = 5, oxidant = 50 mg/L, T = 20 °C

initial RO122 concentration increased, the penetration of photons entering into the solution decreases, so that a rise in its concentration induces an inner filter effect. Consequently, the solution becomes more and more impermeable to UV irradiation. However, the dissociation of peroxides was also reduced, and fewer radicals were produced to react with the target contaminant (Chen et al., 2018; Deng et al., 2013). Secondly, during the destruction of RO122, because of the oxidation of high amount of RO122 with the oxidants, a large number of by-products may be formed. While RO122 with higher initial concentration was introduced into the aqueous solution, more intermediate products may react with reactive radicals, and this may lead to a decrease in radicals' concentration. Among all three processes, removal efficiencies and reaction rate constant values reduced linked to the increase in initial dye concentration due to the fixed amount of oxidant concentration. Similar results were obtained for carbamazepine and antipyrine removal, and studies reported a reduction in PFO kinetic rate constant with the increase in initial pollutant concentration (Deng et al., 2013; Tan et al., 2013).

Effect of initial oxidants concentration

Figure 6 shows the RO122 removal efficiencies for UV/H_2O_2, $UV/S_2O_8^{2-}$, and UV/HSO_5^- processes with different oxidant concentrations. In control experiments using only H_2O_2, $S_2O_8^{2-}$, and HSO_5^-, RO122 removal was identified to be insignificant. For this reason, the effect of interaction between UV and different oxidants on RO122 removal was researched. With the increase of oxidant concentration in the presence of RO122, RO122 removal efficiency increased. At any specific oxidant concentration, the UV/H_2O_2 process had higher RO122 removal than $UV/S_2O_8^{2-}$ and UV/HSO_5^-. While the UV/H_2O_2 process required 90-min reaction duration at 50 mg/L H_2O_2 concentration to provide 95% RO122 removal, it required 60-min, 45-min, and 30-min reaction duration at 100, 150 and 200 mg/L H_2O_2 concentrations, respectively.

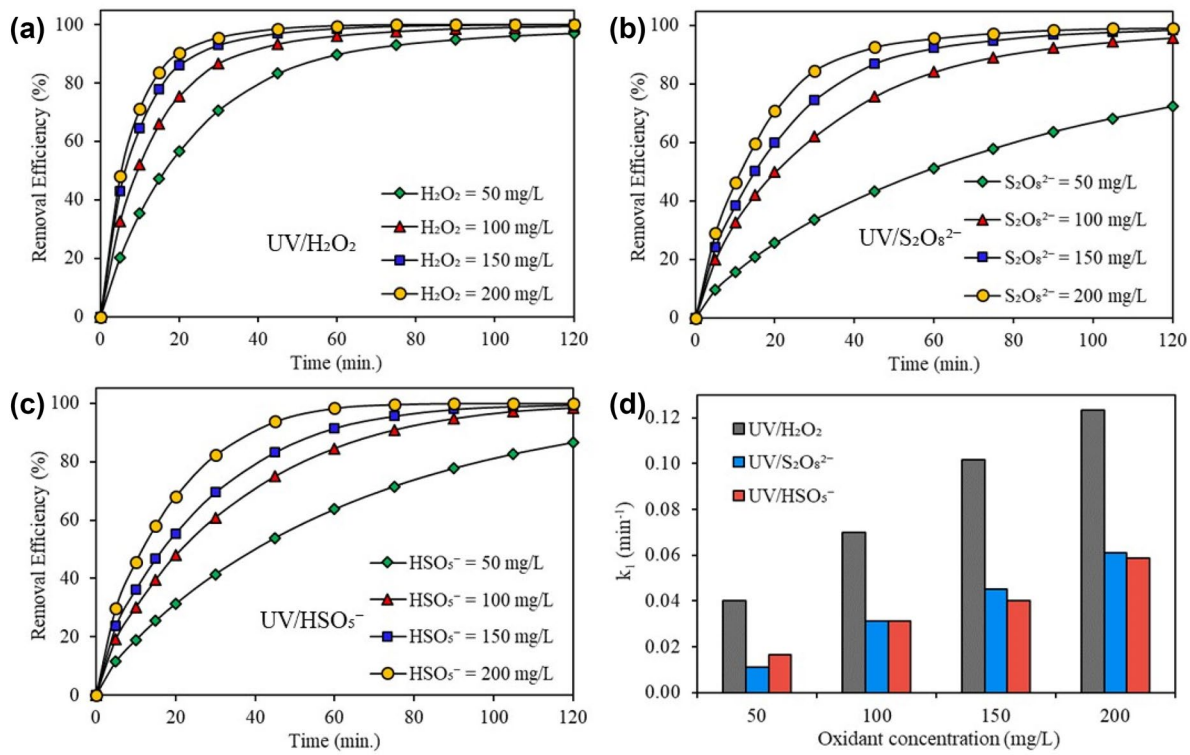

Fig. 6 Effect of oxidant concentration on RO122 removal. **a** UV/H_2O_2, **b** UV/$S_2O_8^{2-}$, **c** UV/HSO_5^-, and **d** the comparison of PFO kinetic rate constant. Experimental conditions: pH = 5, RO122 = 100 mg/L, T = 20 °C

The amount of sulfate and hydroxyl radicals was used to control the removal rate of RO122. With the increasing oxidant concentration (H_2O_2, $S_2O_8^{2-}$, and HSO_5^-), the amount of sulfate and hydroxyl radicals had been increased in UV-based AOPs, and this led to the improved removal rate. Generally, removal rate will be proportional to the amounts of radicals produced at low oxidant concentrations. Additionally, the use of more oxidant may affect removal rates due to the self-scavenging effect (Chen et al., 2018; Deng et al., 2013). In this study, the removal rates increased with the increase in oxidant concentrations used. This shows that the oxidant concentrations used were below the inhibition point. RO122 removal with UV-based AOPs abides PFO kinetics. Independent of the oxidant species used, the PFO kinetic rate constant values displayed a linear correlation with the increase in oxidant concentration (UV/H_2O_2, $k_1 = 0.034[H_2O_2]_0 + 0.801$, $R^2 = 0.994$; UV/$S_2O_8^{2-}$, $k_1 = 0.020[S_2O_8^{2-}]_0 + 0.230$, $R^2 = 0.994$; UV/HSO_5^-, $k_1 = 0.016[HSO_5^-]_0 + 0.178$, $R^2 = 0.984$). Similar results were reported in studies about removal of different organic matter (Gao et al., 2009; Tan et al., 2013).

Effect of different anions on the degradation

Anions such as Cl^-, NO_3^-, and SO_4^{2-} are commonly present in both natural water and wastewater. These anions can scavenge free radicals and can thus affect pollutant removal. Therefore, the effects of Cl^-, NO_3^-, and SO_4^{2-} on the removal of RO122 dye by UV/H_2O_2, UV/$S_2O_8^{2-}$, and UV/HSO_5^- processes were monitored (Fig. 7). The effect of these anions was investigated under the following experimental conditions: a temperature of 20 °C, an initial pH value of 5, an initial RO122 concentration of 100 mg/L, and an initial oxidant concentration of 100 mg/L. An anion concentration of 250 mg/L was used for all compounds investigated. Anion species were found to have a negligible effect on the performance of the UV/H_2O_2 treatment process. In contrast, the presence of

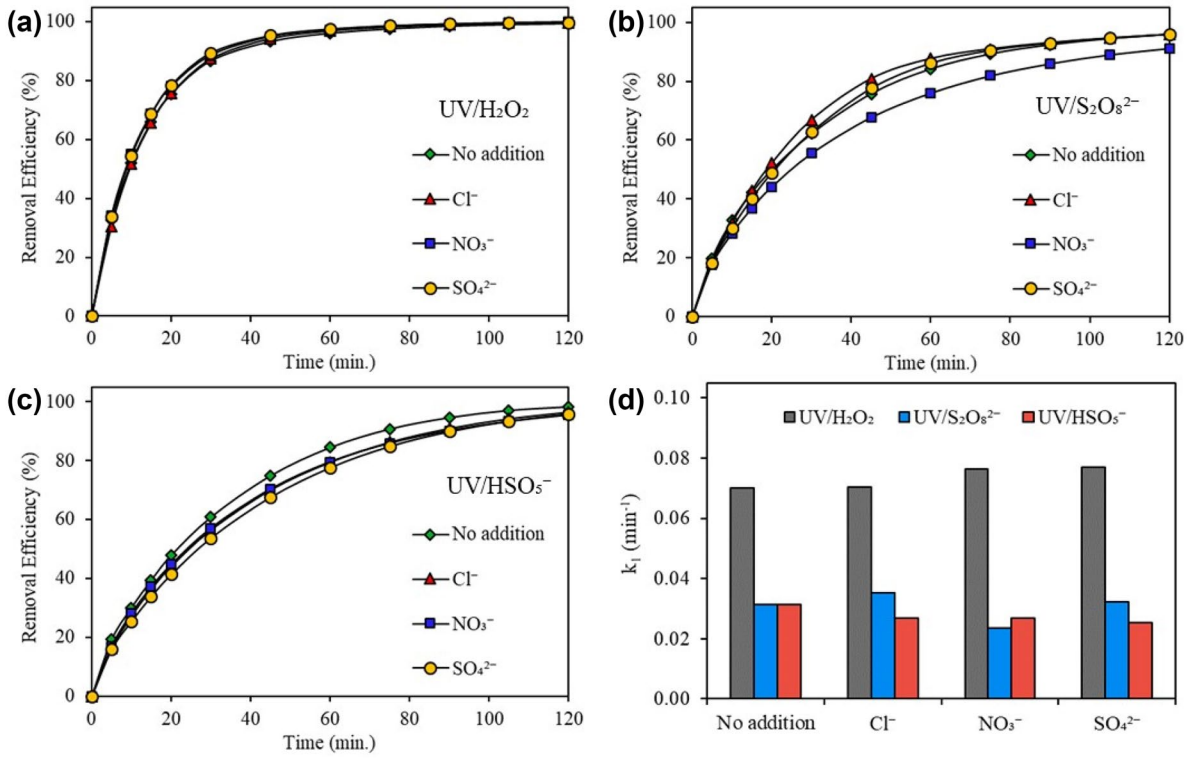

Fig. 7 Effect of different anions on RO122 removal. **a** UV/H_2O_2, **b** $UV/S_2O_8^{2-}$, **c** UV/HSO_5^-, and **d** the comparison of PFO kinetic rate constant. Experimental conditions: pH = 5, RO122 = 100 mg/L, oxidant = 100 mg/L, T = 20 °C

NO_3^- significantly decreased the removal rate of the $UV/S_2O_8^{2-}$ process, while Cl^- and SO_4^{2-} increased the rate of removal. A previous study reported that the formation of reactive chlorine species (e.g., $Cl_2^{\bullet-}$ and $ClHO^{\bullet-}$) at high chlorine doses during the $UV/S_2O_8^{2-}$ treatment process can compensate for the consumption of $SO_4^{\bullet-}$ and even increase the efficiency of the process (Ding et al., 2020). Overall, the removal rate of the $UV/S_2O_8^{2-}$ process was greatest in the presence of Cl^- followed by SO_4^{2-}, while NO_3- reduced the removal rate of the treatment. The addition of Cl^-, NO_3^- and SO_4^{2-} slightly decelerated the removal of RO122 during the UV/HSO_5^- process; this was similar to the results observed when the UV/HSO_5^- process was used in the removal of diethyl phthalate (Lei et al., 2020). The negligible effect of Cl^-, NO_3^-, and SO_4^{2-} may be due to their lower reactivity with free radicals or the formation of secondary radicals such as $SO_4^{\bullet-}$.and $Cl_2^{\bullet-}$.

Effect of solution temperature

Temperature is one of the most important factors affecting reaction rates. Additionally, it is a technique used for H_2O_2, $S_2O_8^{2-}$, and HSO_5^- activation (Devi et al., 2016). For this reason, the RO122 removal was researched over time for the three processes using different solution temperatures. Figure 8 shows the effect of temperature in the interval 10–40 °C at pH 5 for removal of RO122 with UV/H_2O_2, $UV/S_2O_8^{2-}$, and UV/HSO_5^- processes. Temperature encourages formation of hydroxyl radicals from hydrogen peroxide and increases the reactivity of these radicals against pollutants (Sanz et al., 2013). For all three processes, an increase in removal rate was observed as the temperature increased. However, no notable variation was observed for the removal rate with the increase from 30 to 40 °C for the UV/H_2O_2 process. A study of leachate stated that the increase in

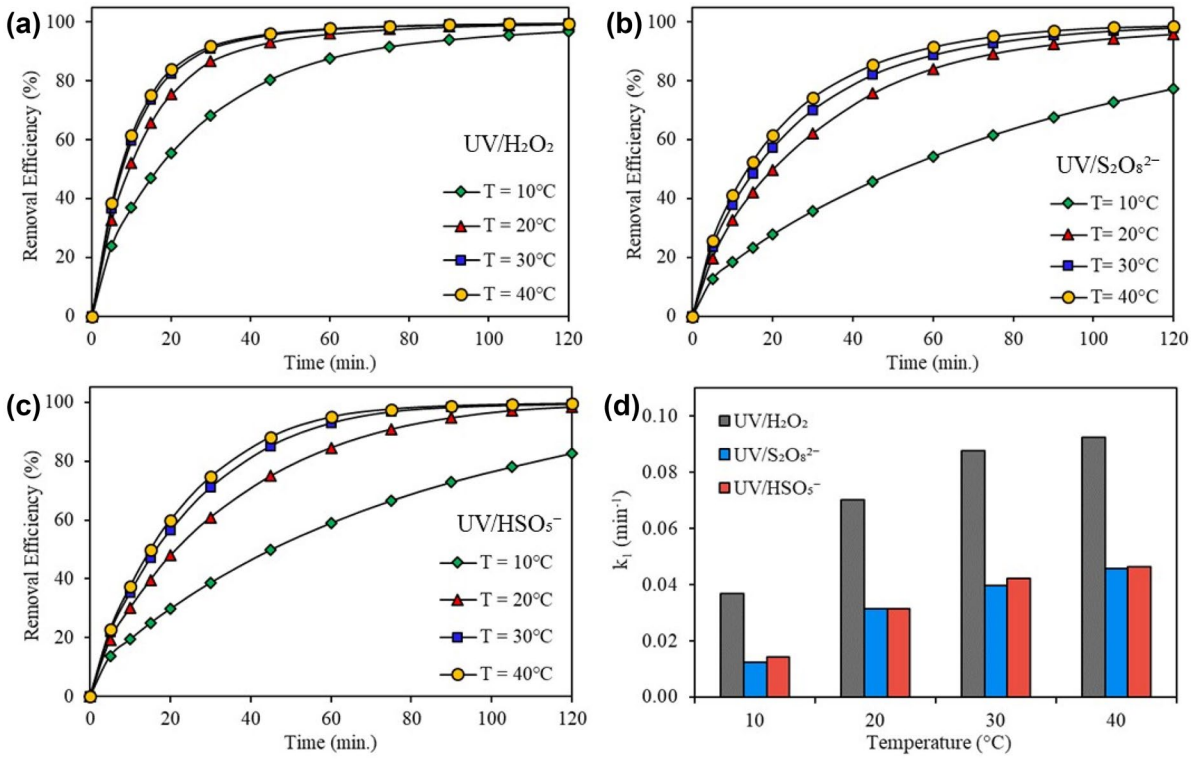

Fig. 8 Effect of temperature on RO122 removal. **a** UV/H_2O_2, **b** $UV/S_2O_8^{2-}$, **c** UV/HSO_5^-, and **d** the comparison of PFO kinetic rate constant. Experimental conditions: RO122 = 100 mg/L, pH = 5, oxidant = 100 mg/L

temperature from 30 to 40 °C increased the degradation rate of H_2O_2. This is because higher temperatures ensure free radical scavenging of H_2O_2, and thus, the concentration of hydroxyl radicals was stated to reduce (Hu et al., 2011). Generally, as the process temperature increased, the separation of H_2O_2, $S_2O_8^{2-}$, and HSO_5^- into $HO^\bullet$ and $SO_4^{\bullet-}$ radicals accelerates. This increases removal of organic pollutants and thus shortens the removal duration.

Economic comparison of the UV/oxidant

Electrical energy is generally the main factor in operating costs for UV-based AOPs (Deng et al., 2013). With the increase in oxidant concentration, the EE/O_{UV} was observed to reduce (Fig. 9). For RO122 removal, EE/O_{UV} values were calculated as 4.67, 9.47, and 9.82 kWh/m^3 for UV/H_2O_2, $UV/S_2O_8^{2-}$, and UV/HSO_5^- systems, respectively, at 200 mg/L oxidant concentration. When oxidant costs are calculated, the $UV/S_2O_8^{2-}$ process had lowest oxidant costs. However, when the total costs (electrical energy and oxidant cost) are calculated, the UV/H_2O_2 process had the lowest cost at all oxidant

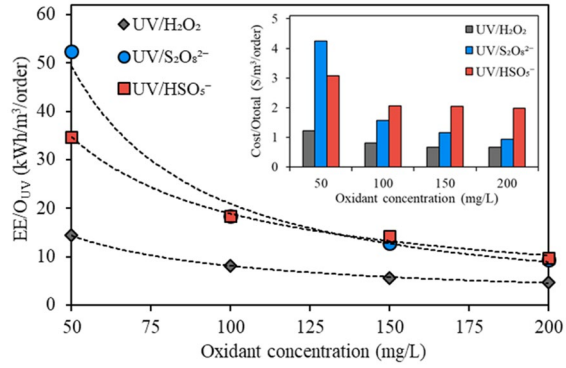

Fig. 9 Economic comparison of UV/H_2O_2, $UV/S_2O_8^{2-}$, and UV/HSO_5^- processes for the removal of RO122. Experimental conditions: RO122 = 100 mg/L, pH = 5, T = 20 °C

concentrations. In terms of total costs, the order was $UV/H_2O_2 > UV/HSO_5^- > UV/S_2O_8^{2-}$ for 50 mg/L oxidant concentration. At higher oxidant concentrations, the order was $UV/H_2O_2 > UV/S_2O_8^{2-} > UV/HSO_5^-$. The results show that AOP using UV/H_2O_2 is the most suitable and economic for RO122 removal. The lowest cost/O_{total} value for the UV/H_2O_2 process was 0.67 \$/m^3/order, while this value was 0.94 and 1.98 \$/m^3/order for $UV/S_2O_8^{2-}$ and UV/HSO_5^- processes, respectively. While the most important finding in the cost analysis is that the $UV/S_2O_8^{2-}$ process is recommended in the existing studies in the literature, the UV/H_2O_2 process is recommended for RO122 removal in this study.

Conclusions

This article assessed RO122 removal with UV/H_2O_2, $UV/S_2O_8^{2-}$, and UV/HSO_5^- processes. The combination of UV with chemical oxidants (H_2O_2, $S_2O_8^{2-}$, and HSO_5^-) improved RO122 removal by a significant degree. At the same oxidant concentration, the UV/H_2O_2 process had better removal performance compared to the $UV/S_2O_8^{2-}$ and UV/HSO_5^- processes. Under all tested conditions, RO122 removal abided well with PFO kinetics. When the effect of solution pH is investigated, the highest rate constant values were obtained at pH 5 for the UV/H_2O_2 process (0.1897 min^{-1}), at pH 7 for the $UV/S_2O_8^{2-}$ process (0.0819 min^{-1}) and at pH 5 for the UV/HSO_5^- process (0.0724 min^{-1}). For the UV/HSO_5^- process, the pH variation had nearly no effect on RO122 removal. A linear correlation was found between the initial oxidant concentration and PFO kinetic rate constant (k_1). The addition of anions was an insignificant impact on the UV/H_2O_2 process; however, it caused inhibition in the UV/HSO_5^- process. RO122 removal rate was determined to increase as temperature increased and reduce as initial RO122 concentration reduced. Energy consumption and cost analysis showed that EE/O_{UV} was the dominant factor for application of the batch advanced oxidation process. Results show that increased oxidant concentration and resulting EE/O_{UV} lowered the total costs of the process. Under the reaction conditions adopted in the study, the UV/H_2O_2 process was concluded to be more economic compared to the other processes linked to total costs of electrical energy and oxidant.

References

Adar, E. (2021). Removal of acid yellow 17 from textile wastewater by adsorption and heterogeneous persulfate oxidation. *International Journal of Environmental Science and Technology, 18*(2), 483–498. https://doi.org/10.1007/s13762-020-02986-5

Alaton, I. A., Balcioglu, I. A., & Bahnemann, D. W. (2002). Advanced oxidation of a reactive dyebath effluent: Comparison of O_3, H_2O_2/UV-C and TiO_2/UV-A processes. *Water Research, 36*(5), 1143–1154. https://doi.org/10.1016/S0043-1354(01)00335-9

Ao, X., & Liu, W. (2017). Degradation of sulfamethoxazole by medium pressure UV and oxidants: Peroxymonosulfate, persulfate, and hydrogen peroxide. *Chemical Engineering Journal, 313*, 629–637. https://doi.org/10.1016/j.cej.2016.12.089

Azam, A., & Hamid, A. (2006). Effects of gap size and UV dosage on decolorization of C.I. Acid Orange 7 by UV/H2O2 process. *Journal of Hazardous Materials*, *133*(1–3), 167–171. https://doi.org/10.1016/j.jhazmat.2005.10.005

Bakht Shokouhi, S., Dehghanzadeh, R., Aslani, H., & Shahmahdi, N. (2020). Activated carbon catalyzed ozonation (ACCO) of Reactive Blue 194 azo dye in aqueous saline solution: Experimental parameters, kinetic and analysis of activated carbon properties. *Journal of Water Process Engineering, 35*, 101188. https://doi.org/10.1016/j.jwpe.2020.101188

Balapure, K., Bhatt, N., & Madamwar, D. (2015). Mineralization of reactive azo dyes present in simulated textile waste water using down flow microaerophilic fixed film bioreactor. *Bioresource Technology, 175*, 1–7. https://doi.org/10.1016/j.biortech.2014.10.040

Beltrán, F. J., González, M., & González, J. F. (1997). Industrial wastewater advanced oxidation. Part 1. UV radiation in the presence and absence of hydrogen peroxide. *Water Research*, *31*(10), 2405–2414. https://doi.org/10.1016/S0043-1354(97)00077-8

Blackburn, R. S. (2004). Natural polysaccharides and their interactions with dye molecules: Applications in effluent treatment. *Environmental Science and Technology, 38*(18), 4905–4909. https://doi.org/10.1021/es049972n

Bolton, J. R., Bircher, K. G., Tumas, W., & Tolman, C. A. (2001). Figures-of-merit for the technical development and application of advanced oxidation technologies for both electric- and solar-driven systems. *Pure and Applied Chemistry, 73*(4), 627–637. https://doi.org/10.1351/pac200173040627

Bolton, J. R., Stefan, M. I., Shaw, P.-S., & Lykke, K. R. (2011). Determination of the quantum yields of the potassium ferrioxalate and potassium iodide–iodate actinometers and a method for the calibration of radiometer detectors. *Journal of Photochemistry and Photobiology a: Chemistry, 222*(1), 166–169. https://doi.org/10.1016/j.jphotochem.2011.05.017

Cai, A., Deng, J., Zhu, T., Ye, C., Li, J., Zhou, S., Li, Q., & Li, X. (2021). Enhanced oxidation of carbamazepine by UV-LED/persulfate and UV-LED/H_2O_2 processes in the presence of trace copper ions. *Chemical Engineering Journal, 404*, 127119. https://doi.org/10.1016/j.cej.2020.127119

Cao, J., Sanganyado, E., Liu, W., Zhang, W., & Liu, Y. (2019). Decolorization and detoxification of Direct Blue 2B by

indigenous bacterial consortium. *Journal of Environmental Management, 242*, 229–237. https://doi.org/10.1016/j.jenvman.2019.04.067

Chen, L., Cai, T., Cheng, C., Xiong, Z., & Ding, D. (2018). Degradation of acetamiprid in UV/H_2O_2 and UV/persulfate systems: A comparative study. *Chemical Engineering Journal, 351*, 1137–1146. https://doi.org/10.1016/j.cej.2018.06.107

Cui, M. H., Cui, D., Liang, B., Sangeetha, T., Wang, A. J., & Cheng, H. Y. (2016). Decolorization enhancement by optimizing azo dye loading rate in an anaerobic reactor. *RSC Advances, 6*, 49995–50001. https://doi.org/10.1039/c6ra04665g

De Gisi, S., & Notarnicola, M. (2017). Industrial Wastewater Treatment. In Abraham, M. A., *Encyclopedia of Sustainable Technologies* (pp. 23–42). Elsevier. https://doi.org/10.1016/B978-0-12-409548-9.10167-8

Değermenci, G. D. (2021). Removal of reactive azo dye using platinum-coated titanium electrodes with the electro-oxidation process. *Desalination and Water Treatment, 218*, 436–443. https://doi.org/10.5004/dwt.2021.26981

Deng, J., Shao, Y., Gao, N., Xia, S., Tan, C., Zhou, S., & Hu, X. (2013). Degradation of the antiepileptic drug carbamazepine upon different UV-based advanced oxidation processes in water. *Chemical Engineering Journal, 222*, 150–158. https://doi.org/10.1016/j.cej.2013.02.045

Devi, P., Das, U., & Dalai, A. K. (2016). In-situ chemical oxidation: Principle and applications of peroxide and persulfate treatments in wastewater systems. *Science of the Total Environment, 571*, 643–657. https://doi.org/10.1016/j.scitotenv.2016.07.032

Dhaka, S., Kumar, R., Lee, S., & hun, Kurade, M. B., & Jeon, B. H. (2018). Degradation of ethyl paraben in aqueous medium using advanced oxidation processes: Efficiency evaluation of UV-C supported oxidants. *Journal of Cleaner Production, 180*, 505–513. https://doi.org/10.1016/j.jclepro.2018.01.197

Ding, D., Liu, C., Ji, Y., Yang, Q., Chen, L., Jiang, C., & Cai, T. (2017). Mechanism insight of degradation of norfloxacin by magnetite nanoparticles activated persulfate: Identification of radicals and degradation pathway. *Chemical Engineering Journal, 308*, 330–339. https://doi.org/10.1016/j.cej.2016.09.077

Ding, X., Gutierrez, L., Croue, J. P., Li, M., Wang, L., & Wang, Y. (2020). Hydroxyl and sulfate radical-based oxidation of RhB dye in UV/H_2O_2 and UV/persulfate systems: Kinetics, mechanisms, and comparison. *Chemosphere, 253*, 126655. https://doi.org/10.1016/j.chemosphere.2020.126655

Dionysiou, D. D., Suidan, M. T., Baudin, I., & Laîné, J. M. (2004). Effect of hydrogen peroxide on the destruction of organic contaminants-synergism and inhibition in a continuous-mode photocatalytic reactor. *Applied Catalysis b: Environmental, 50*(4), 259–269. https://doi.org/10.1016/j.apcatb.2004.01.022

Ferreira, S. A. D., Donadia, J. F., Gonçalves, G. R., Teixeira, A. L., Freitas, M. B. J. G., Fernandes, A. A. R., & Lelis, M. F. F. (2019). Photocatalytic performance of granite waste in the decolorization and degradation of Reactive Orange 122. *Journal of Environmental Chemical Engineering, 7*(3), 103144. https://doi.org/10.1016/j.jece.2019.103144

Franca, R. D. G., Vieira, A., Carvalho, G., Oehmen, A., Pinheiro, H. M., Crespo, M. T. B., & Lourenco, N. D. (2020). Oerskovia paurometabola can efficiently decolorize azo dye Acid Red 14 and remove its recalcitrant metabolite. *Ecotoxicology and Environmental Safety, 191*, 110007. https://doi.org/10.1016/j.ecoenv.2019.110007

Ganesh, R., Boardman, G. D., & Michelsen, D. (1994). Fate of azo dyes in sludges. *Water Research, 28*(6), 1367–1376. https://doi.org/10.1016/0043-1354(94)90303-4

Gao, N., & yun, Deng, Y., & Zhao, D. (2009). Ametryn degradation in the ultraviolet (UV) irradiation/hydrogen peroxide (H_2O_2) treatment. *Journal of Hazardous Materials, 164*(2–3), 640–645. https://doi.org/10.1016/j.jhazmat.2008.08.038

Guo, H. X., Lin, K. L., Zheng, Z. S., Xiao, F. B., & Li, S. X. (2012). Sulfanilic acid-modified P25 TiO_2 nanoparticles with improved photocatalytic degradation on Congo red under visible light. *Dyes and Pigments, 92*(3), 1278–1284. https://doi.org/10.1016/j.dyepig.2011.09.004

He, X., Mezyk, S. P., Michael, I., Fatta-Kassinos, D., & Dionysiou, D. D. (2014). Degradation kinetics and mechanism of β-lactam antibiotics by the activation of H_2O_2 and $Na_2S_2O_8$ under UV-254 nm irradiation. *Journal of Hazardous Materials, 279*, 375–383. https://doi.org/10.1016/j.jhazmat.2014.07.008

Hu, X., Wang, X., Ban, Y., & Ren, B. (2011). A comparative study of UV-Fenton, UV-H2O2 and Fenton reaction treatment of landfill leachate. *Environmental Technology, 32*(9), 945–951. https://doi.org/10.1080/09593330.2010.521953

Kausar, A., Shahzad, R., Asim, S., BiBi, S., Iqbal, J., Muhammad, N., Sillanpaa, M., & Din, I. U. (2021). Experimental and theoretical studies of Rhodamine B direct dye sorption onto clay-cellulose composite. *Journal of Molecular Liquids, 328*, 115165. https://doi.org/10.1016/j.molliq.2020.115165

Kermani, M., Farzadkia, M., Morovati, M., Taghavi, M., Fallahizadeh, S., Khaksefidi, R., & Norzaee, S. (2020). Degradation of furfural in aqueous solution using activated persulfate and peroxymonosulfate by ultrasound irradiation. *Journal of Environmental Management, 266*, 110616. https://doi.org/10.1016/j.jenvman.2020.110616

Khan, J. A., He, X., Shah, N. S., Khan, H. M., Hapeshi, E., Fatta-Kassinos, D., & Dionysiou, D. D. (2014). Kinetic and mechanism investigation on the photochemical degradation of atrazine with activated H_2O_2, $S_2O_8^{2-}$ and HSO_5^-. *Chemical Engineering Journal, 252*, 393–403. https://doi.org/10.1016/j.cej.2014.04.104

Kishor, R., Purchase, D., Saratale, G. D., Ferreira, L. F. R., Bilal, M., Iqbal, H. M. N., & Bharagava, R. N. (2021). Environment friendly degradation and detoxification of Congo red dye and textile industry wastewater by a newly isolated Bacillus cohnni (MW406977). *Environmental Technology & Innovation, 22*, 101425. https://doi.org/10.1016/j.eti.2021.101425

Klavarioti, M., Mantzavinos, D., & Kassinos, D. (2009). Removal of residual pharmaceuticals from aqueous systems by advanced oxidation processes. *Environment International, 35*(2), 402–417. https://doi.org/10.1016/j.envint.2008.07.009

Kolthoff, I. M., & Miller, I. K. (1951). The Chemistry of Persulfate. I. The Kinetics and Mechanism of the Decomposition of the Persulfate Ion in Aqueous Medium. *Journal of the American Chemical Society*, *73*(7), 3055–3059. https://doi.org/10.1021/ja01151a024

Lee, Y. M., Lee, G., & Zoh, K. D. (2021). Benzophenone-3 degradation via UV/H_2O_2 and UV/persulfate reactions. *Journal of Hazardous Materials, 403*, 123591. https://doi.org/10.1016/j.jhazmat.2020.123591

Lei, Y., Lu, J., Zhu, M., Xie, J., Peng, S., & Zhu, C. (2020). Radical chemistry of diethyl phthalate oxidation via UV/peroxymonosulfate process: Roles of primary and secondary radicals. *Chemical Engineering Journal, 379*, 122339. https://doi.org/10.1016/j.cej.2019.122339

Li, W., Jain, T., Ishida, K., & Liu, H. (2017). A mechanistic understanding of the degradation of trace organic contaminants by UV/hydrogen peroxide, UV/persulfate and UV/free chlorine for water reuse. *Environmental Science: Water Research and Technology, 3*, 128–138. https://doi.org/10.1039/c6ew00242k

Liang, C., Wang, Z. S., & Bruell, C. J. (2007). Influence of pH on persulfate oxidation of TCE at ambient temperatures. *Chemosphere, 66*(1), 106–113. https://doi.org/10.1016/j.chemosphere.2006.05.026

Liu, X., Liu, Y., Lu, S., Wang, Z., Wang, Y., Zhang, G., Guo, X., Guo, W., Zhang, T., & Xi, B. (2020). Degradation difference of ofloxacin and levofloxacin by UV/H_2O_2 and UV/PS (persulfate): Efficiency, factors and mechanism. *Chemical Engineering Journal, 385*, 123987. https://doi.org/10.1016/j.cej.2019.123987

Liu, Y., He, X., Fu, Y., & Dionysiou, D. D. (2016). Degradation kinetics and mechanism of oxytetracycline by hydroxyl radical-based advanced oxidation processes. *Chemical Engineering Journal, 284*, 1317–1327. https://doi.org/10.1016/j.cej.2015.09.034

Mahmoud, M. E., Khalifa, M. A., El-Mallah, N. M., Hassouba, H. M., & Nabil, G. M. (2021). Performance of MnO_2 nanoparticles-coated cationic CTAB for detoxification and decolorization of sulfonated remazol red and reactive black 5 dyes from water. *International Journal of Environmental Science and Technology*. https://doi.org/10.1007/s13762-021-03153-0

Malakootian, M., Mansoorian, H. J., Hosseini, A., & Khanjani, N. (2015). Evaluating the efficacy of alumina/carbon nanotube hybrid adsorbents in removing Azo Reactive Red 198 and Blue 19 dyes from aqueous solutions. *Process Safety and Environmental Protection, 96*, 125–137. https://doi.org/10.1016/j.psep.2015.05.002

Meerbergen, K., Crauwels, S., Willems, K. A., Dewil, R., Van Impe, J., Appels, L., & Lievens, B. (2017). Decolorization of reactive azo dyes using a sequential chemical and activated sludge treatment. *Journal of Bioscience and Bioengineering, 124*(6), 668–673. https://doi.org/10.1016/j.jbiosc.2017.07.005

Oturan, M. A., & Aaron, J. J. (2014). Advanced oxidation processes in water/wastewater treatment: Principles and applications. A review. *Critical Reviews in Environmental Science and Technology., 44*, 2577–2641. https://doi.org/10.1080/10643389.2013.829765

Pearce, C. I., Lloyd, J. R., & Guthrie, J. T. (2003). The removal of colour from textile wastewater using whole bacterial cells: A review. *Dyes and Pigments., 58*(3), 179–196. https://doi.org/10.1016/S0143-7208(03)00064-0

Peng, Y., Fu, D., Liu, R., Zhang, F., & Liang, X. (2008). $NaNO_2$/$FeCl_3$ catalyzed wet oxidation of the azo dye Acid Orange 7. *Chemosphere, 71*(5), 990–997. https://doi.org/10.1016/j.chemosphere.2007.10.065

Pérez-Calderón, J., Santos, M. V., & Zaritzky, N. (2020). Synthesis, characterization and application of cross-linked chitosan/oxalic acid hydrogels to improve azo dye (Reactive Red 195) adsorption. *Reactive and Functional Polymers, 155*, 104699. https://doi.org/10.1016/j.reactfunctpolym.2020.104699

Qi, C., Liu, X., Ma, J., Lin, C., Li, X., & Zhang, H. (2016). Activation of peroxymonosulfate by base: Implications for the degradation of organic pollutants. *Chemosphere, 151*, 280–288. https://doi.org/10.1016/j.chemosphere.2016.02.089

Ravadelli, M., da Costa, R. E., Lobo-Recio, M. A., Akaboci, T. R. V., Bassin, J. P., Lapolli, F. R., & Belli, T. J. (2021). Anoxic/oxic membrane bioreactor assisted by electrocoagulation for the treatment of azo-dye containing wastewater. *Journal of Environmental Chemical Engineering, 9*(4), 105286. https://doi.org/10.1016/j.jece.2021.105286

Rehman, F., Sayed, M., Khan, J. A., Shah, N. S., Khan, H. M., & Dionysiou, D. D. (2018). Oxidative removal of brilliant green by UV/$S_2O_8^{2-}$, UV/HSO_5^- and UV/H_2O_2 processes in aqueous media: A comparative study. *Journal of Hazardous Materials, 357*, 506–514. https://doi.org/10.1016/j.jhazmat.2018.06.012

Rodrigues de Almeida, E. J., Christofoletti Mazzeo, D. E., Deroldo Sommaggio, L. R., Marin-Morales, M. A., Rodrigues de Andrade, A., & Corso, C. R. (2019). Azo dyes degradation and mutagenicity evaluation with a combination of microbiological and oxidative discoloration treatments. *Ecotoxicology and Environmental Safety, 183*, 109484. https://doi.org/10.1016/j.ecoenv.2019.109484

Santos, S. C. R., & Boaventura, R. A. R. (2016). Adsorption of cationic and anionic azo dyes on sepiolite clay: Equilibrium and kinetic studies in batch mode. *Journal of Environmental Chemical Engineering, 4*(2), 1473–1483. https://doi.org/10.1016/j.jece.2016.02.009

Sanz, J., Lombraña, J. I., & de Luis, A. (2013). Temperature-assisted UV/H2O2 oxidation of concentrated linear alkylbenzene sulphonate (LAS) solutions. *Chemical Engineering Journal, 215–216*, 533–541. https://doi.org/10.1016/j.cej.2012.09.133

Saratale, R. G., Saratale, G. D., Chang, J. S., & Govindwar, S. P. (2009). Ecofriendly degradation of sulfonated diazo dye C.I. Reactive Green 19A using Micrococcus glutamicus NCIM-2168. *Bioresource Technology*, *100*(17), 3897–3905. https://doi.org/10.1016/j.biortech.2009.03.051

Siegrist, R. L., Crimi, M., & Simpkin, T. J. (2011). In situ chemical oxidation for groundwater remediation. *Springer*. https://doi.org/10.1007/978-1-4419-7826-4

Sirajudheen, P., Nikitha, M. R., Karthikeyan, P., & Meenakshi, S. (2020). Perceptive removal of toxic azo dyes from water using magnetic Fe_3O_4 reinforced graphene oxide–carboxymethyl cellulose recyclable composite: Adsorption investigation of parametric studies and their mechanisms. *Surfaces and Interfaces, 21*, 100648. https://doi.org/10.1016/j.surfin.2020.100648

Tan, C., Gao, N., Deng, Y., Zhang, Y., Sui, M., Deng, J., & Zhou, S. (2013). Degradation of antipyrine by UV, UV/H_2O_2 and UV/PS. *Journal of Hazardous Materials, 260*, 1008–1016. https://doi.org/10.1016/j.jhazmat.2013.06.060

Wang, F., Wang, W., Yuan, S., Wang, W., & Hu, Z. H. (2017). Comparison of UV/H_2O_2 and UV/PS processes for the degradation of thiamphenicol in aqueous solution. *Journal of Photochemistry and Photobiology a: Chemistry, 348*, 79–88. https://doi.org/10.1016/j.jphotochem.2017.08.023

Yang, S., Yang, X., Shao, X., Niu, R., & Wang, L. (2011). Activated carbon catalyzed persulfate oxidation of Azo dye acid orange 7 at ambient temperature. *Journal of Hazardous Materials, 186*(1), 659–666. https://doi.org/10.1016/j.jhazmat.2010.11.057

Zhan, B. J., Li, J. S., Xuan, D. X., & Poon, C. S. (2020). Recycling hazardous textile effluent sludge in cement-based construction materials: Physicochemical interactions between sludge and cement. *Journal of Hazardous Materials, 381*, 121034. https://doi.org/10.1016/j.jhazmat.2019.121034

Zhang, T., Chen, Y., Wang, Y., Le Roux, J., Yang, Y., & Croué, J. P. (2014). Efficient peroxydisulfate activation process not relying on sulfate radical generation for water pollutant degradation. *Environmental Science and Technology, 48*(10), 5868–5875. https://doi.org/10.1021/es501218f

Zhang, Y., Zhang, J., Xiao, Y., Chang, V. W. C., & Lim, T. T. (2016). Kinetic and mechanistic investigation of azathioprine degradation in water by UV, UV/H_2O_2 and UV/persulfate. *Chemical Engineering Journal, 302*, 526–534. https://doi.org/10.1016/j.cej.2016.05.085

Zhao, C., Pelaez, M., Duan, X., Deng, H., O'Shea, K., Fatta-Kassinos, D., & Dionysiou, D. D. (2013). Role of pH on photolytic and photocatalytic degradation of antibiotic oxytetracycline in aqueous solution under visible/solar light: Kinetics and mechanism studies. *Applied Catalysis b: Environmental, 134–135*, 83–92. https://doi.org/10.1016/j.apcatb.2013.01.003